Adv. Composite Mater., Vol. 14, No. 2, pp. 147–164 (2005)

Also available online - www.vsppub.com

Passive wireless strain monitoring of a tire using capacitance and electromagnetic induction change

RYOSUKE MATSUZAKI *,†, AKIRA TODOROKI, HIDEO KOBAYASHI and YOSHINOBU SHIMAMURA

Department of Mechanical Sciences and Engineering, Tokyo Institute of Technology, Japan

Received 20 May 2004; accepted 4 November 2004

Abstract—Strain monitoring of tires in-service of automobiles is quite effective for improving reliability of tires and an anti-lock braking system (ABS). A previous study by the authors presented a new wireless strain monitoring method that adopts the tire itself as a sensor with an oscillator circuit. This method is simple and useful, but it requires a battery to activate the oscillator circuit. The present study proposes and investigates a new passive wireless strain measurement system using capacitance change of tires. The system consists of external antennas and strain sensor with an inductance-capacitance (LC) resonant circuit. This wireless system uses electromagnetic coupling between two inductors of the antenna and the sensor. This method allows use of a part of an actual tire as a capacitor of the LC circuit. Tire deformation changes the sensor's resonant frequency. This resonant frequency change is measured as a change in the phase angle of the antenna using electromagnetic induction. Tensile tests are performed and the antenna phase angles are measured during the tests. Consequently, experiments show that this method is effective for passive wireless strain monitoring of tires.

Keywords: Passive; wireless; strain; monitoring; tire; sensor; electric capacitance; electromagnetic induction.

1. INTRODUCTION

Automobile safety is increasingly important. Smart tires are currently under development to prevent tire bursting [1–7]. Most smart tires have integrated or attached sensors to measure deformation or internal pressure of tires during

*To whom correspondence should be addressed at Room 473, Building #1, Ishikawadai, Tokyo Institute of Technology, 2-12-2 Ookayama, Meguro-ku, Tokyo, 152-8552, Japan. E-mail: rmatsuza@ginza.mes.titech.ac.jp

†This paper is a translation of an original Japanese-language paper: Ryosuke Matsuzaki, Akira Todoroki, Hideo Kobayashi, Yoshinobu Shimamura, Passive Wireless Strain Monitoring of Tire using Capacitance and Electromagnetic Induction change, *J. Japan Soc. Compos. Mater.* **30** (4) (2004).

their typically long periods of service. Pohl *et al*. [1] have reported a smart tire that has an embedded pin connected to a surface acoustic wave (SAW) sensor to measure tire-tread rubber deformation. The embedded sensor enables highly precise measurement of road surface friction. That precise friction measurement enables a more efficient anti-lock braking system (ABS). This information also allows the early detection of tire-tread separation, which is an important threat to automobile safety [2].

Several specifications are necessary for tire sensors to be installed in smart tires. First, wireless monitoring is indispensable because a tire usually rotates, thereby making it difficult to use wired sensors. Second, because tire rubber has low stiffness, embedding or attaching the sensors can easily disturb the stress profile or cause tire deformation: sensors should not cause such disturbances. Third, the large difference of stiffness of sensors from the rubber may cause debonding between the sensors and the rubber over their long periods of use: the stiffness difference should be small. Fourth, because the tire itself is not an expensive product, the sensor must be inexpensive.

Most sensors employed for the smart tires sacrifice one or two of those requisite specifications. For example, micro-electro-mechanical systems (MEMS) for wireless strain measurement are embedded to create smart composite structures [8]. The wireless MEMS includes a sensor, a signal processing unit, and an antenna. The wireless MEMS strain sensor is an attractive product, but embedding the MEMS sensor into a tire is not recommended because of the large difference of stiffness between the sensor and the rubber tire. Such large difference in stiffness may cause deformation and stress disturbances; it may also engender debonding between sensors and rubber over a long period of service.

Conventional strain gages also pose similar problems to those of wireless MEMS. A small wireless data transfer tip can be applied to conventional strain gages to transfer data wirelessly. Even for the strain gage, however, the large stiffness difference and weak bonding between the strain gage and the rubber may cause debonding over a long period of service. High cost sensor systems, such as optical fiber systems [9], are not feasible because a tire itself is not an expensive product. Therefore, a novel sensor is demanded for a true ‘smart tire’.

Tires are composed of rubber with carbon black, steel wire, and organic fiber. Steel wire belts are inserted under the tread rubber. The steel wire itself is an electric conductive material; the rubber is a dielectric material. This tire structure is quite similar to an electrical condenser, comprising a couple of electrodes and an intervening dielectric material. Tire deformation changes the spacing between the steel wires, which implies a change in capacitance of the tire part. Measuring the capacitance change of the tire thereby indicates the tire strain or deformation without the need for additional embedded or attached sensors.

A previous study [10] proposed a new strain measurement method. This previous method measured, wirelessly, the change of electrical capacitance during tire deformation. The previous method employed a capacitance resistance (CR)

oscillating circuit to wirelessly transfer the capacitance change information. The steel wire of the tires was adopted as an electrode of the CR oscillating circuit. Tire deformation caused an electrical capacitance change in the circuit, which changed the oscillating frequency. Measurement of the frequency change in the oscillating circuit indicated, wirelessly, the strain of the deformed tire. The previous system was applied to a rectangular specimen made from a truck tire. Then, static tension tests, cyclic loading tests and feasibility tests were performed. The previous wireless strain measurement system adopted the tire itself as a sensor. Therefore, the system causes no problems like those mentioned before. However, the system requires batteries to activate the CR oscillating circuit. This fact may cause some drawbacks for long-term service.

The present study improves the previous method for wireless tire monitoring to produce a passive wireless sensor. It requires no batteries to activate the sensor circuit. A specimen made from a commercially available tire is connected to an inductance-capacitance (LC) resonant circuit as a capacitance. The system consists of an external antenna and a strain sensor, LC resonant circuit to which a tire is connected. The wireless system uses electromagnetic coupling between two inductors of the antenna and the strain sensor. When the specimen deforms, the specimen capacitance changes. That capacitance change then alters the strain sensor's resonant frequency. That resonant frequency change is measured as a change in the phase angle of the antenna using electromagnetic induction. This new passive wireless method is applied to a specimen and the static applied strain is measured.

2. MONITORING SYSTEM

This wireless, passive strain-measurement system employs the tire itself as a sensor. Figure 1 shows the inner structure of a typical radial tire. For a radial tire, the direction of the carcass fiber is the radial direction of the tire. Usually, the carcass

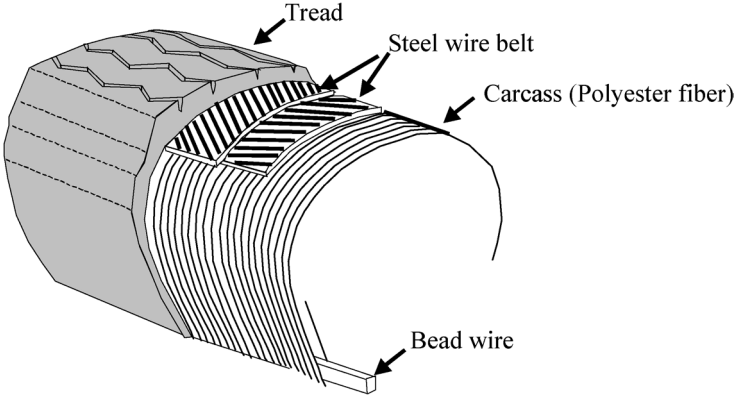

Figure 1. The inner structure of a steel-wire-reinforced radial tire.

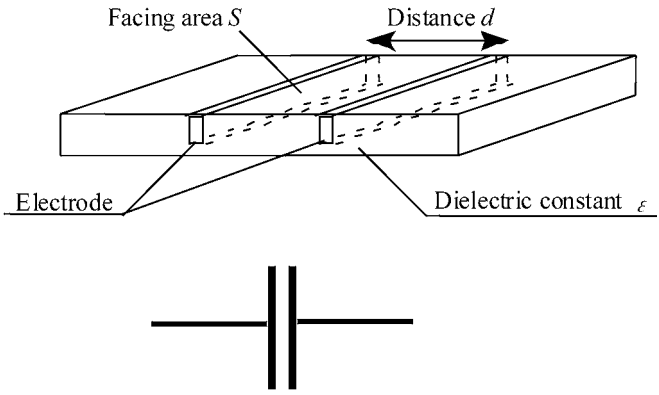

Figure 2. Condenser model of a steel wire belt of a tire.

fiber is made from organic fibers, such as polyester fibers. Steel wire layers are mounted as cross-ply laminates of composite materials on the carcass fiber layer. These fibers are covered with rubber; then the tread rubber layer is mounted on the steel wire layers, as shown in Fig. 1. Tread deformation is transferred to the steel wire layers. This fact means that measuring of the strain of the steel wire layer reveals the tire-tread deformation.

In the steel wire layer, the steel wire is a straight electrical conductive material and the rubber is dielectric material. Consider a couple of adjacent steel wires, like those shown in Fig. 2. In that figure, a couple of steel wires are placed face-to-face. Then the dielectric rubber is inserted between the two steel wires. Electric voltage is charged between the steel wires. This structure forms an electrical condenser. The adjacent steel wires form the electrodes of an electric condenser. The electrical capacitance of the condenser is calculated as

$$C = \varepsilon \frac{S}{d}, \tag{1}$$

where ε is a dielectric constant of the rubber, S, is the electrode area; d is the spacing between the adjacent steel wires. When the steel wire layer is elongated, the spacing d is increased: from equation (1), this size increase reduces the capacitance. Shrinking the steel wire layer increases the capacitance. The consequent tire deformation changes the electrical capacitance of the tire.

Harpster *et al*. [11] have proposed a passive wireless humidity sensor consisting of a capacitive humidity sensor chip and a hybrid coil. These passive sensors require no batteries to activate the sensor circuit. In this study, a passive, wireless humidity-sensor system proposed by Harpster *et al*. is improved to produce the tire strain-measurement system used in this study. Figure 3 shows a schematic representation of the passive wireless strain-measurement system. This system comprises an external antenna and a strain sensor. A tire belt is connected to the strain sensor circuit as a capacitance. Wireless communication between the external antenna and

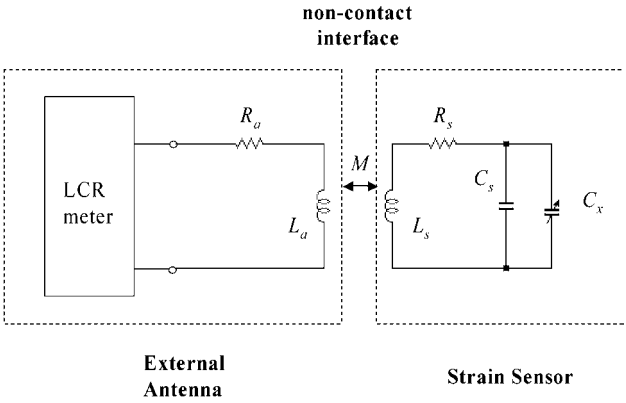

Figure 3. Circuit model of wireless passive sensor using electromagnetic induction change.

a strain sensor is performed by means of the electromagnetic induction between them.

As shown in Fig. 3, the strain sensor circuit is a typical LC resonant circuit. Impedance of the strain sensor circuit, $Z_s(\omega)$, is

$$Z_s(\omega) = R_s + j\left\{\omega L_s - \frac{1}{\omega(C_s + C_x)}\right\}, \tag{2}$$

where j is $\sqrt{-1}$, ω is radian frequency, L_s is an inductance of the coil of the sensor circuit, R_s is a series resistance of the coil L_s, C_s is a capacitance of the sensor circuit and C_x is the tire specimen capacitance.

From equation (2), the resonant frequency, f_r, of the strain sensor circuit is calculated as

$$f_r = \frac{1}{2\pi\sqrt{L_s(C_s + C_x)}}. \tag{3}$$

In the LC resonant circuit, a condenser C_x, which is one of the two essential parts needed to calculate the resonant frequency, is replaced with the tire specimen. Therefore, the tire electrical capacitance changes when the tire deforms. That capacitance change engenders change of the resonant frequency, f_r, of the strain sensor when inductance, L_s, is fixed. Measurement of the change of the resonant frequency, f_r, indicates the tire capacitance change attributable to tire deformation.

Figure 4 shows the equivalent circuit used to model the sensor system shown in Fig. 3. The impedance of the external antenna, $Z_a(\omega)$, is given as

$$Z_a(\omega) = R_a + j\omega L_a + \frac{\omega^2 M^2}{Z_s(\omega)}, \tag{4}$$

where L_a is the inductance of the coil of the antenna circuit, R_a is a series resistance of the coil L_a and M is a mutual inductance between coil L_a and L_s.

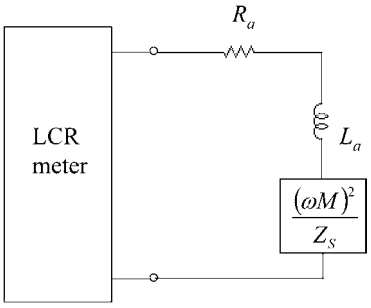

Figure 4. Equivalent circuit model of wireless passive sensor.

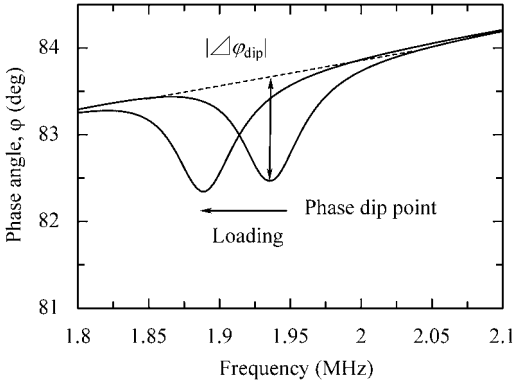

Figure 5. Shift of phase dip point caused by tensile loading of tire.

From equations (2) and (4), the impedance of the external antenna at the resonant frequency, ω_0, of the strain sensor is calculated as

$$Z_{\mathrm{a}}(\omega_0) = R_{\mathrm{a}} + j\omega_0 L_{\mathrm{a}} + \frac{\omega_0^2 M^2}{R_{\mathrm{s}}}. \tag{5}$$

Figure 5 shows the typical angle phase of the antenna, $\varphi(f)$, for measuring frequency f: the phase dip minimum point occurs at the resonant frequency f_{r}. The frequency at the phase dip minimum point of the antenna impedance is independent of the mutual induction M and equal to the resonant frequency, f_{r}, of the strain sensor.

The impedance phase dip magnitude $|\Delta\varphi_{\mathrm{dip}}|$ is the difference in $\varphi(\omega_0)$ between a coupled (M = finite) and uncoupled ($M = 0$) antenna as follows.

$$|\Delta\varphi_{\mathrm{dip}}| = |\angle(R_{\mathrm{a}} + j\omega_0 L_{\mathrm{a}}) - \angle Z_{\mathrm{a}}(\omega_0)| \cong \tan^{-1}\left(\frac{\omega_0 M^2}{L_{\mathrm{a}} R_{\mathrm{s}}}\right). \tag{6}$$

The quality factor Q_{s}, the sharpness of the resonant, is as follows.

$$Q_{\mathrm{s}} = \frac{1}{R_{\mathrm{s}}}\sqrt{\frac{L_{\mathrm{s}}}{C_{\mathrm{s}} + C_x}}. \tag{7}$$

From this equation, minimizing R_s and maximizing L_s increase Q_s. Their change also increases the antenna impedance and the magnitude of the phase dip. Higher-Q_s sensors are desired because it is thereby easy to find the phase-dip-minimum point from the sharp phase angle peaks. Higher-Q_s sensors, therefore, enable us to measure the capacitance change at longer testing distance between the strain sensor and the external antenna.

This monitoring system offers three main advantages. Firstly, the tire itself is adopted as a sensor: this feature prevents debonding of the sensor and disturbance of the stress and deformation field of the tire over its long period of service. Secondly, the strain sensor system is a passive wireless type. Such a passive wireless sensor requires no batteries to activate the sensor circuit. Thereby, weight reduction and long-term stabilization are assured. Thirdly, a monitoring system using electromagnetic induction is not affected by mutual induction, M, and changed distance between the external antenna and the strain sensor.

3. MEASUREMENT OF ELECTRICAL CAPACITANCE CHANGE

3.1. Experimental procedure

The specimen employed in the present study is taken from a commercially available radial tire. The proposed system can be applied as an attached or embeddable patch, like a strain gage, instead of using the actual steel wires of a radial tire. The patch-type system is similar to a conventional strain gage. Using the actual steel wires of the tire can be more effective to measure tire deformation. For this reason, more trials will be undertaken in future work.

Figure 6 shows the specimen configuration. The specimen length, width, and thickness are 270, 30, and 4 mm, respectively. The longitudinal direction of the specimen is the circumferential direction of the tire. In this specimen, steel wires of diameter of 1.0 mm are embedded in parallel in spacing of about 2.5 mm. The fiber angle is about $\pm 20°$ to the longitudinal direction of the specimen. The steel wire surface is covered with a special surface treatment to improve the bonding between steel and rubber. For this study, the wire is polished with a sheet of sandpaper

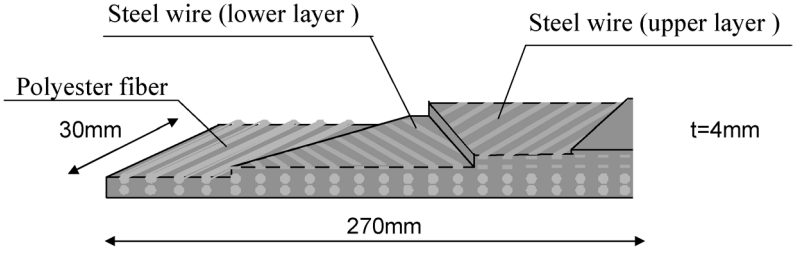

Figure 6. Specimen configuration.

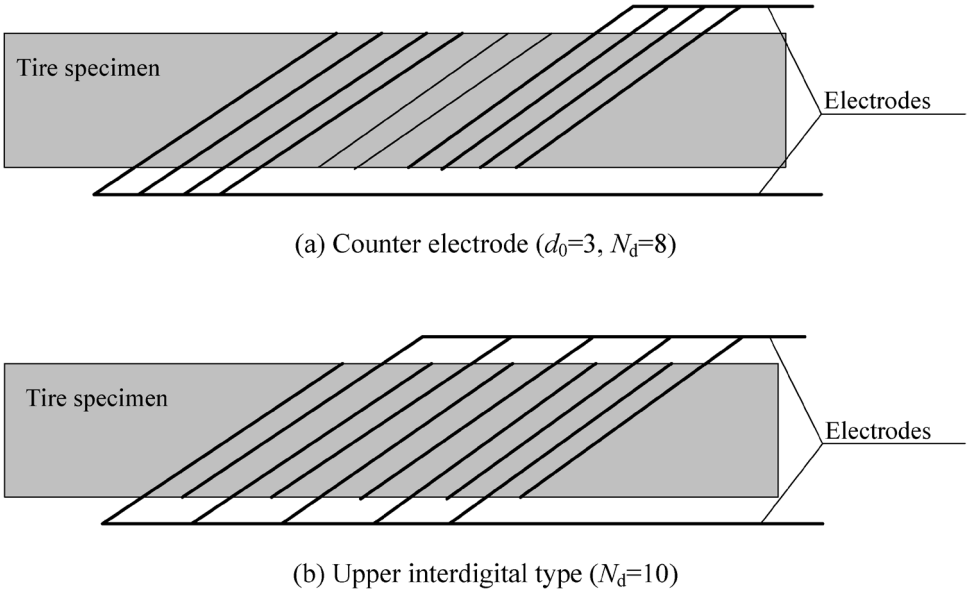

Figure 7. Electrodes alignment.

to remove this surface treatment. After polishing, two lead wires are soldered to the steel wires to produce two electrodes. A conventional strain gage designed for rubber is attached to the specimen surface between the two electrodes. It measures the applied strain.

Two layers of steel wires (±20°) exist in the tire specimen (see Fig. 6). Three types of electrode alignment are proposed: upper layer, lower layer, and upper and lower layer. 'Upper layer type' uses steel wires embedded in upper steel wire layer of the specimen, as shown in Fig. 7a. 'Lower layer type' uses the steel wires embedded in lower steel wire layer of the specimen. The 'Upper and lower layer type' use steel wires embedded in upper and lower steel wire layers from the specimen as two electrodes.

The use of interdigital electrodes is proposed to increase the tire's capacitance change attributable to applied strain, as shown in Fig. 7b. There are two types of interdigital electrodes: upper interdigital and lower interdigital. 'Upper interdigital type' has interdigital electrodes in upper steel wire layer of the tire specimen and 'lower interdigital type' has interdigital electrodes in lower steel wire layer of the tire specimen.

Firstly, static tension tests are performed to measure the capacitance change of the specimen during loading and unloading. Figure 8 shows the experimental setup: a tensile testing machine produced by Shimadzu, an LCR meter (LCR meter no 3522) produced by E.E. Hioki, a tire specimen, and a computer. For measurement, the charged alternating current is 100 kHz. The applied strain is also measured with a conventional strain gage attached to the specimen surface. Tensile tests are performed at stroke speed of 1.0 mm/min and up to 3 mm of displacement.

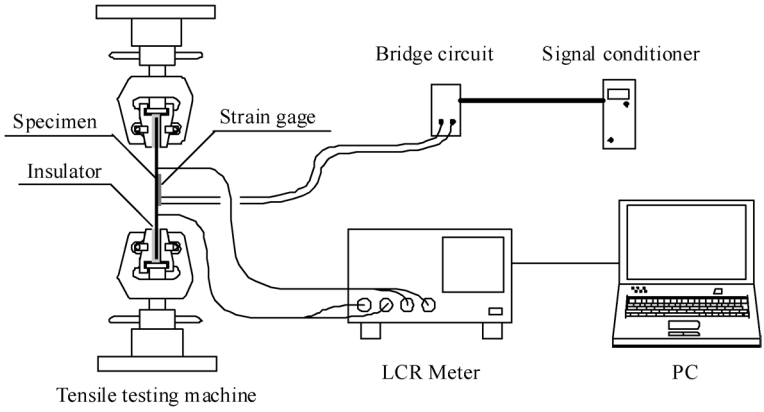

Figure 8. Experimental set-up for capacitance change measurement.

Unloading is performed after tensile testing. Electrical capacitance is measured without stopping loading. A silicone rubber sheet is inserted between the jig and the specimen to prevent short-circuit between the specimen and the testing machine jigs.

Secondly, the initial capacitance at the no-loading condition, C_0, and capacitance change with the strain change from 0 $\mu\varepsilon$ to 3000 $\mu\varepsilon$, ΔC, of the tire specimen are measured with the change of initial distance between two electrodes on the no-loading condition, d_0, or the number of electrodes, N_d. The initial distance between electrodes, d_0, is normalized by the distance between adjacent wires: 4 mm.

Finally, aligning the interdigital electrodes, the initial capacitance on the no-loading condition, C_0, and capacitance change, ΔC, of the tire specimen are measured with the change in the number of interdigital electrodes, N_d.

3.2. Capacitance change caused by applied strain

Figure 9 shows results of the capacitance change of the tire specimen (upper layer type: $d_0 = 1$, $N_\mathrm{d} = 2$) caused by tensile loading. The abscissa is the applied strain measured with the attached strain gage; the ordinate is the measured capacitance change of the specimen. This figure reveals that the capacitance increases with the increase of tensile loading from about 18 to 27 pF. From equation (1), the increase of the capacitance indicates the decrease of the spacing distance between the steel wires during tensile loading. This decreased distance can be explained using Fig. 10. Because the steel fiber angle is about 20°, the tensile loading causes wire rotation, as shown in Fig. 10. This rotation decreases the wire angle. In addition, the transverse compressive strain decreases the specimen width. These in turn decrease spacing during tensile loading. Although there is a small hysteresis loop of the measured capacitance during loading and unloading, its effect is negligible for monitoring tire strain.

Figure 11 shows the frequency response characteristic of the tire specimen capacitance. The abscissa is the frequency of the charged alternating current; the ordinate is the measured capacitance and phase angle of the specimen impedance.

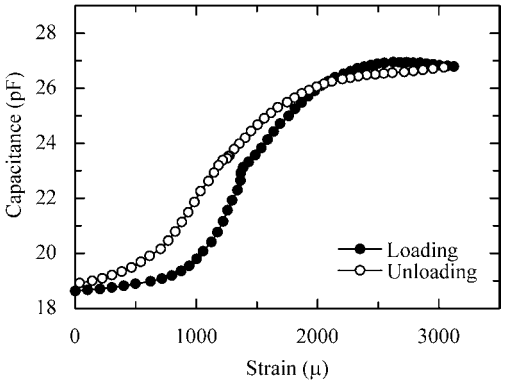

Figure 9. Measured capacitance change during loading and unloading (upper layer type).

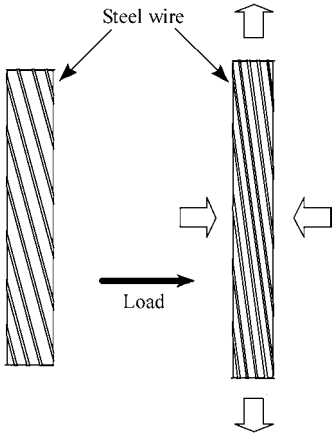

Figure 10. Schema of spacing decrease with the increase of tensile load.

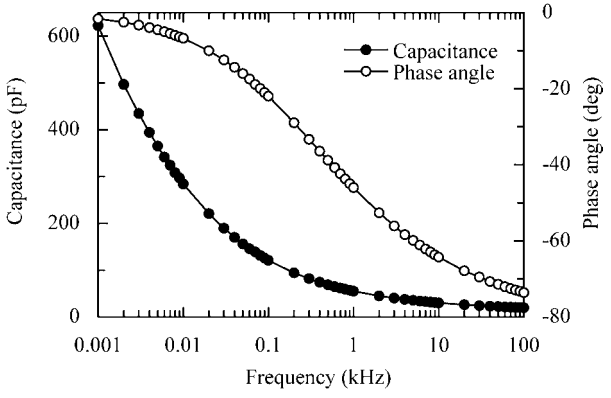

Figure 11. Measured frequency response of the capacitance and phase angle of tires (upper layer type).

This figure shows that the phase angle decreases and becomes near $-90°$ with the increased frequency. Therefore, the tire specimen can be regarded as an electrical condenser in the high frequency range. Qualitatively, the same results are obtained in cases of the other electrode alignments: lower layer type, upper and lower layer type, upper interdigital type, and lower interdigital type.

3.3. Initial distance between electrodes, d_0

Figures 12 and 13 show results of initial capacitance, C_0, and capacitance change, ΔC, with the change of initial normalized distance between electrodes, d_0, respectively. The abscissa is the initial distance between electrodes, d_0, and the ordinate is the initial capacitance, C_0, in Fig. 12 and capacitance change, ΔC, in Fig. 13. In the upper layer type (solid circle symbol) and lower layer type (open circle symbol), C_0 and ΔC decrease with the increase of d_0, as shown in Figs 12 and 13. These results agree with equation (1): the increase of the distance between electrodes, d,

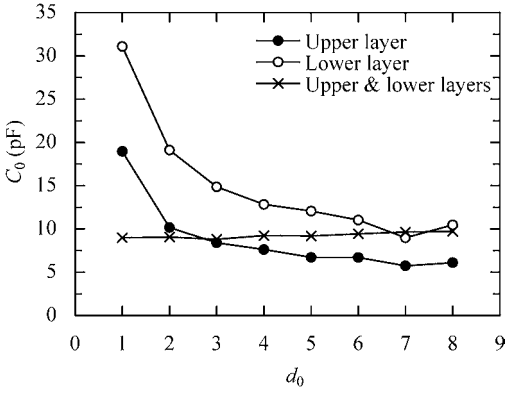

Figure 12. Measured relationship between initial capacitance and spacing d_0 for three different types.

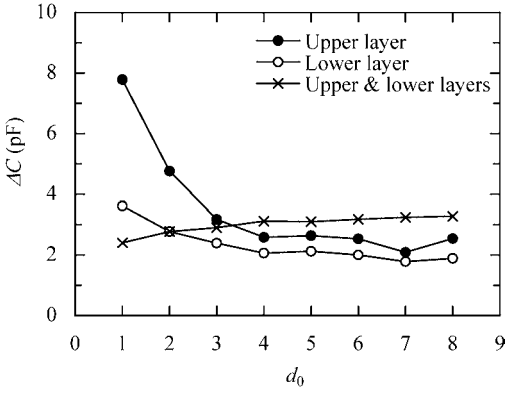

Figure 13. Measured relationship between capacitance change and spacing d_0 for three different types.

decreases the capacitance, C. Although C_0 of the upper layer type is smaller than that of the lower layer type, ΔC of the upper layer type is larger than that of the lower layer type.

3.4. Number of electrodes, N_d

Figures 14 and 15 show results of the initial capacitance, C_0, and capacitance change, ΔC, with the change of the number of electrodes, N_d, respectively. The abscissa shows the number of electrodes, N_d; the ordinate shows the initial capacitance, C_0, in Fig. 14 and capacitance change, ΔC, in Fig. 15. In all three different types — the upper layer type (solid circle symbol), lower layer type (open circle symbol) and upper and lower layer type (cross symbol) — the value of C_0 increases with increased N_d, as shown in Fig. 14. Increasing N_d indicates an increased number of capacitors in the tire specimen, which implies increased C_0.

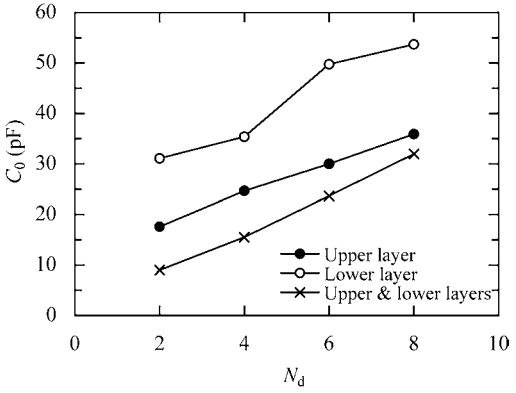

Figure 14. Measured relationship between initial capacitance and number of wires N_d for three different types.

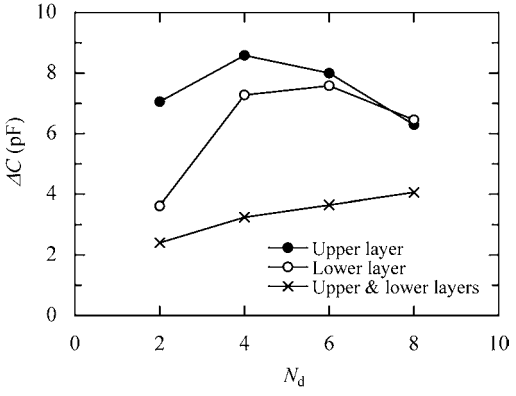

Figure 15. Measured relationship between capacitance change and number of wires N_d for three different types.

Although C_0 of the upper layer type is smaller than that of the lower layer type, ΔC of the upper layer type is larger than that of the lower layer type.

3.5. Interdigital electrodes

Figures 16 and 17 show results of the initial capacitance, C_0, and capacitance change, ΔC, with the change of the number of interdigital electrodes, N_d, respectively. The abscissa is the number of electrodes, N_d, and the ordinate is the initial capacitance, C_0 in Fig. 16 and capacitance change, ΔC, in Fig. 17. These figures reveal that C_0 and ΔC drastically increase with the increase of N_d. The cause of this result is similar to that for results shown in Figs 14 and 15. The ΔC of the upper interdigital type (solid circle symbol) is twice as large as that of the lower interdigital type (open circle symbol).

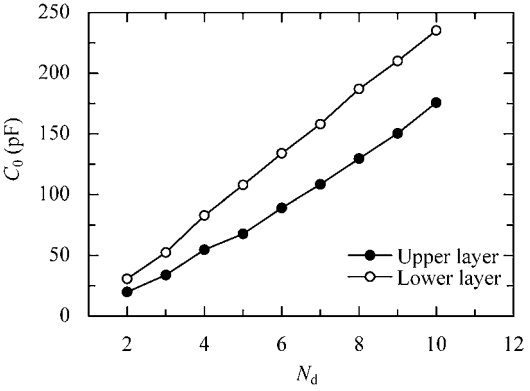

Figure 16. Measured relationship between initial capacitance and of number of wires N_d for two different types of interdigital electrodes.

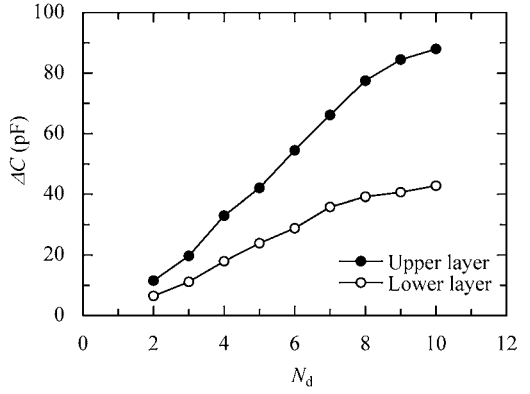

Figure 17. Measured relationship between capacitance change and number of wires N_d for two different types of interdigital electrodes.

A large-ΔC sensor is desired because such a sensor offers high resolution of the measured strain. Consequently, the upper interdigital type ($N_d = 10$) allows production of a specimen of very large ΔC. The N_d is set the maximum limit at 10 in this study to prevent increase of the sensing area.

4. TENSILE TESTS USING WIRELESS PASSIVE SENSOR

4.1. Experimental procedure

Static tensile tests using the sensor are performed to check the feasibility of this wireless passive monitoring system. Table 1 lists experimental values for the antenna circuit coil inductance (L_a) and the strain sensor circuit (L_s). A ceramic condenser of 0.01 μF is used as the constant condenser C_s. Figure 18 shows the experimental setup of the tensile testing machine, tire specimen, strain sensor, external antenna, LCR meter, and computer. Static tension tests are performed to measure frequency response characteristic of the phase angle of the antenna circuit impedance, φ.

The proposed passive sensor assumes a pure electrical capacitance as a sensing target. However, the tire specimen capacitance is not a pure capacitance. Therefore, before using the tire specimen, a ceramic condenser, a pure electrical capacitance, is used as the capacitance C_x: $C_x = 2000$ pF; 4000 pF. The frequency response characteristic of the phase angle, φ, is measured with the change of distance d_i to confirm the effect of the distance between two coils of the antenna circuit and strain sensor circuit, d_i. Using the tire specimen (upper interdigital type: $N_d = 10$) as a capacitance C_x of the strain sensor circuit, static tension tests are performed at stroke speed of 1.0 mm/min and up to 3 mm of displacement. Subsequently, unloading is performed. The electrical capacitance is measured without stopping the loading. A silicone rubber sheet is inserted between the jig and the specimen to prevent electrical shorts between the specimen and the testing machine jigs.

Table 1.
Measured coil parameters

	L_a	L_s
Length (mm)	2.69	18.2
Number of windings	5	19
Diameter of coil (mm)	6.56	6.56
Diameter of wire (mm)	0.600	0.600
Measured L (nH)	188	725
Calculated (nH)	248	670
Resistance (Ω)	0.331	0.214

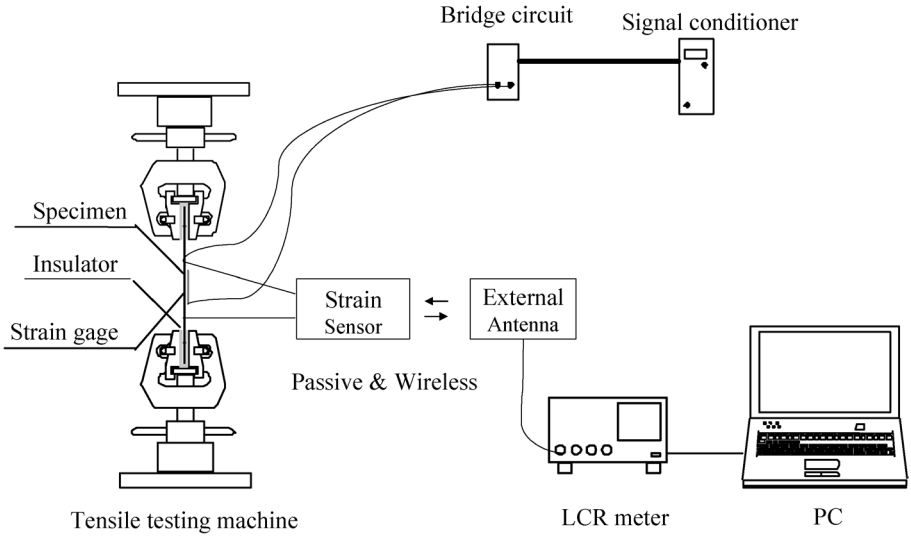

Figure 18. Experimental set-up for tensile test with wireless passive sensor.

4.2. Result and discussion

Figure 19 shows the frequency response characteristic of phase angle, φ, using the ceramic condenser as a condenser C_x: $C_x = 0$, 2000 and 4000 pF. In this figure, the abscissa is the measuring frequency of the LCR meter and the ordinate is the measured phase angle, φ, of the external antenna impedance. As shown in this figure, the phase dip minimum point observed at resonant frequency, f_r, decreases with the increase of capacitance C_x, which agrees with equation (3). Figure 20 shows results of the frequency response characteristic of the phase angle, φ, with the change of distance between two coils, d_i. The figure reveals that, although the phase dip magnitude $|\Delta\varphi_{dip}|$ decreases with the increase of d_i, the measured frequency at phase dip minimum point is independent of d_i and equal to the resonant frequency.

Figure 21 shows the results of the frequency response characteristic of the phase angle, φ, and impedance of the antenna circuit, Z_a, using the tire specimen as a condenser C_x on no-loading condition. The abscissa is the measuring frequency of the LCR meter and the ordinate is the measured impedance, Z_a: (solid circle symbol), and its phase angle, φ: (open circle symbol), of the external antenna impedance. This figure confirms that the phase angle, φ, has a dip minimum point at the resonant frequency (2.2 MHz).

Figure 22 shows results of static tension tests of tire specimen using the proposed wireless passive system. In this figure, the abscissa is the loading strain measured by means of attached strain gage and the ordinate is the measured resonant frequency, f_r, obtained from the frequency at the phase dip minimum point of φ. These static tension tests are performed twice: first loading (solid circle symbol), first unloading (open circle symbol), second loading (solid triangle symbol), and second unloading (open triangle symbol). The measured resonant frequency, f_r, decreases with the

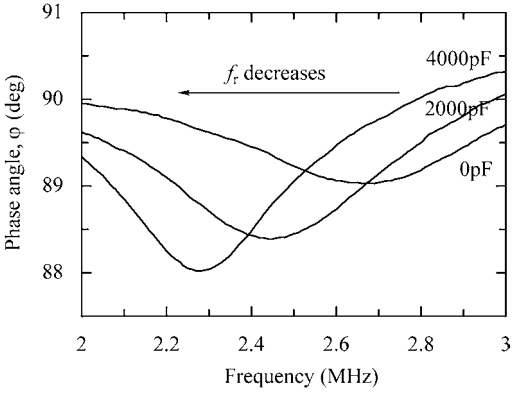

Figure 19. Measured phase angle change with capacitance change ($C_x = 0$ pF; 2000 pF; 4000 pF).

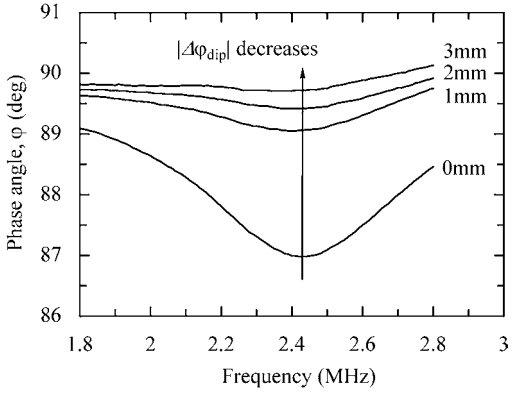

Figure 20. Measured phase angle change with distance change ($d_i = 0$ mm; 1 mm; 2 mm; 3 mm).

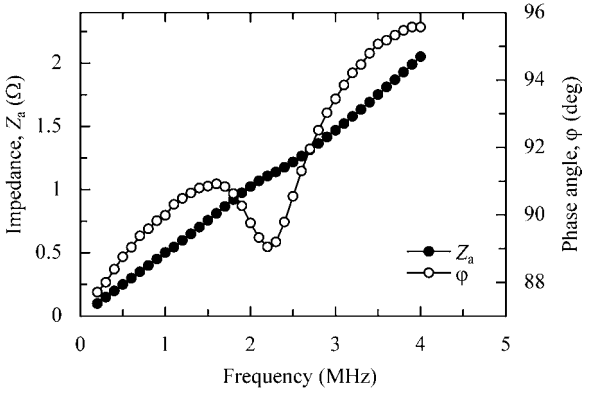

Figure 21. Measured Z_a and φ of antenna impedance of wireless passive sensor using tire as C_x.

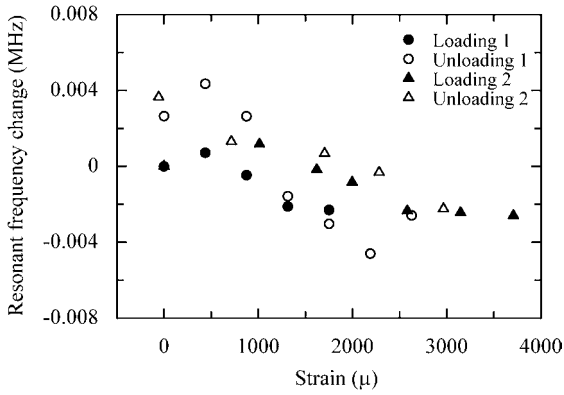

Figure 22. Measured relationship between strain and resonant frequency of wireless passive sensor.

increase in the tensile strain, as shown in Fig. 22, corresponding to the increase of capacitance occurring with the increase in tensile strain, as shown in Fig. 9. Results obtained from Fig. 22 indicate that the proposed method is applicable for wireless strain measurement of commercially available tires.

The data scatter observed in Fig. 22 is caused by the LCR-meter performance. Because the maximum measuring frequency of the LCR meter is limited less than 5 MHz, the resonant frequency, f_r, of the sensor circuit must also be less than 5 MHz. To set the resonant frequency, f_r, under this limit, the sensor circuit needs the condenser as C_s of 0.01 μF, in parallel with the tire specimen. Consequently, the change of the resonant frequency resulting from the capacitance change of the tire specimen is only about 4 kHz. This makes it difficult to measure the change of the phase dip minimum point precisely. A measuring device measures impedances at a higher frequency range. Therefore, a condenser C_s to reduce the resonant frequency is not necessary. Thereby, this problem will be improved.

In practical use, the strain sensor is embedded in a tire and an external antenna is located on an axle. In this case, the radio range, i.e. the distance between a strain sensor and an external antenna, is about 300 mm. This means that the measurable distance, at present 5 mm, is insufficient. Therefore, the coil configuration requires improvement to obtain a longer wireless range, as implied by equation (7).

Another difficulty is that the measuring the impedance requires about 2 min at current condition, which renders dynamic measurement difficult. However, this problem will be improved by means of a rapid and sensitive impedance-measurement device.

5. CONCLUSIONS

The present study proposed a novel passive wireless method to measure tire strain. Because the method employs the tire itself as a sensor and does not require additional sensors, it does not disturb the tire stress and deformation field.

Moreover, it does not cause sensor debonding. Steel wires of the tire are adopted as electrodes to charge high-frequency alternating current. Tire deformation causes a change of the tire's electrical capacitance. The tire is connected to a simple LC resonant circuit as condenser and the capacitance change of the tire is converted to resonant frequency change of the LC resonant circuit. The method was applied to a rectangular specimen cut from a commercially available radial tire and was investigated experimentally. We reached the following conclusions.

(1) Electrical capacitance of the tire increases with increased tensile loading. This increase of capacitance is caused by the decrease of the spacing of those wires under tension loading. Capacitance measurement of the tire specimen indicated an appropriate alignment setup of electrodes.

(2) This new wireless passive strain-measurement method uses capacitance change of tire itself. The tire is connected to the LC resonant circuit as a condenser. Then, the resonant frequency changes as a result of the altered tire capacitance. The proposed passive wireless strain-measurement system was experimentally demonstrated with static tension tests. It was verified to be effective.

REFERENCES

1. M. Brandt, V. Bachmann, A. Vogt, M. Fach, K. Mayer, B. Breuer and H. L. Hartnagel, Highly sensitive AlGaAs/GaAs position sensors for measurement of tyre tread deformation, *Electron. Lett.* **34**, 760–762 (1998).
2. A. Pohl, R. Steindl and L. Reindl, The 'intelligent tire' utilizing passive SAW sensors-measurement of tire friction, *IEEE Trans. Instrum. Meas.* **48**, 1041–1046 (1999).
3. K. Mnif, A smart tire pressure monitoring system, *Sensors* **18**, 40–46 (2001).
4. O. Yilmazoglu, M. Brandt, J. Sigmund, E. Genc and H. L. Hartnagel, Integrated InAs/GaSb 3D magnetic field sensors for 'the intelligent tire', *Sens. Actuators A* **94**, 59–63 (2001).
5. T. Umeno, K. Asano, H. Ohashi, M. Yonetani, T. Naitou and T. Taguchi, Observer-based estimation of parameter variations and its application to tyre pressure diagnosis, *Control Eng. Pract.* **9**, 639–645 (2001).
6. N. Persson, S. Ahlqvist, U. Forssell and F. Gustafsson, Low tire pressure warning system using sensor fusion, in: *SAE Conf. Proc.*, pp. 77–79 (1999).
7. A. Gavine, Common sense? The latest in vehicle safety comes courtesy of continental with its potentially life-saving tread deformation sensor, *Tire Technol. Int.* (September), 32–33 (2001).
8. C. Hautamaki, S. Zurn, S. C. Mantell and D. L. Polla, Experimental evaluation of MEMS strain sensors embedded in composites, *J. Microelectromech. Syst.* **8**, 272–279 (1999).
9. M. E. Palmer, C. C. Boyd, J. McManus and S. Meller, Wireless smart-tire for road friction measurement and self state determination, in: *Proc. 43rd AIAA/ASME/ASCE/AHS/ASC Structures, Structural Dynamics, and Materials Conference, AIAA*, AIAA2002, p. 1548 (2002).
10. R. Matsuzaki, A. Todoroki, H. Kobayashi and Y. Shimamura, Wireless strain monitoring of tire using capacitance change with oscillator, *J. Japan Soc. Compos. Mater.* **30**, 55–62 (2004).
11. T. J. Harpster, B. Stark and K. Najafi, A passive wireless integrated humidity sensor, *Sens. Actuators A*, **95**, 100–107 (2002).